Molecular Dynamics at the Receptor Level of Immunodominant Myelin Oligodendrocyte Glycoprotein 35-55 Epitope Implicated in Multiple Sclerosis

Mary Patricia Yannakakis[1], Haralambos Tzoupis[1], Elena Michailidou[1], Efthimia Mantzourani[2], Carmen Simal[1], Theodore Tselios[1,*]

[1] Department of Chemistry, University of Patras, GR-26504, Rion, Patras, Greece

[2] Cardiff University, Cardiff School of Pharmacy, CF10 3NB, Wales

*Corresponding author: Tel: +302610 997905; Fax: +302610 997180; email: ttselios@upatras.gr

Abstract

Multiple Sclerosis (MS) is a common autoimmune disease whereby myelin is destroyed by the immune system. The disease is triggered by the stimulation of encephalitogenic T-cells *via* the formation of a trimolecular complex between the Human Leukocyte Antigen (HLA), an immunodominant epitope of myelin proteins and T-cell Receptor (TCR). Myelin Oligodendrocyte Glycoprotein (MOG) is located on the external surface of myelin and has been implicated in MS induction. The immunodominant 35-55 epitope of MOG is widely used for *in vivo* biological evaluation and immunological studies that are related with chronic Experimental Autoimmune Encephalomyelitis (EAE, animal model of MS), inflammatory diseases and MS. In this report, Molecular Dynamics (MD) simulations were used to explore the interactions of the MOG_{35-55} at the receptor level. A detailed mapping of the developed interactions during the creation of the trimolecular complex is reported. This is the first attempt to gain an understanding of the molecular recognition of the MOG_{35-55} epitope by the HLA and TCR receptors. During the formation of the trimolecular complex, the residues Arg^{41} and Arg^{46} of MOG_{35-55} have been confirmed to serve as TCR anchors while Tyr^{40} interacts with HLA. The present structural findings indicate that the Arg at positions 41 and 46 is a key residue for the stimulation of the encephalitogenic T-cells.

Keywords: Bioactive conformation; Molecular Dynamics; Multiple Sclerosis (MS); Myelin Oligodendrocyte Glycoprotein (MOG); Human Leukocyte Antigen (HLA); T-cell Receptor (TCR)

1. Introduction

Multiple Sclerosis (MS) is the most common autoimmune disease of the Central Nervous System (CNS) in which a coordinated attack of the immune system against myelin takes place. [1, 2] Myelin Basic Protein (MBP), Proteolipid Protein (PLP), Myelin Oligodendrocyte Glycoprotein (MOG) and Myelin-Associated Glycoprotein (MAG) are the main myelin proteins in the CNS and they have been recognized as putative auto-antigens for MS.[3] MS onset is triggered by the activation of the encephalitogenic T-cells through the formation of a trimolecular complex between the T-cell receptor (TCR), the peptide (antigen) -with identical residue sequence to a fragment of a protein of the myelin sheath (molecular mimicry theory)[4, 5]- and the Major Histocompatibility Complex (MHC) or Human Leukocyte Antigen (HLA). The ability of the peptide-HLA complex to activate T-cells is correlated with the strength of its binding affinity with TCR.[6-8] Conversely, stimulation or not of T-cells that are responsible for MS follows.[9-13] The HLA class II receptors are dimers comprised of two different polypeptide chains (α and β).[14, 15] In this class of macromolecules the polypeptide chains are joined together, creating a single receptor for the antigens to bind to. Subsequently, the newly formed complex is recognized by the receptors on the surface of T-cells. The formation of the trimolecular complex leads to the activation of the T-cells through a cascade of biochemical changes and the induction of the immune response to the antigen. The TCR is also composed of two different polypeptide chains. The two chains comprising the TCR (α and β), include variable domains called Complementarity Determining Regions (CDRs). These domains are implicated in the recognition process between the TCR and the HLA-antigen complex.[16] The diversity of the CDRs plays a crucial role in the recognition of the different antigens as they are presented by the HLA receptors. The CDRs comprising the TCR chains are very effective at screening the various antigens

presented to the T-cells.[9, 17] It has been estimated by *in vivo* experiments that the TCR unique structures in humans are over >2.5x10^7.[17, 18] Despite the diverse numbers and the rigorous selection process of T-cells in the thymus,[19, 20] there are cases where the selection process fails to single out T-cells reacting to self-antigens.[21] Thus, the failure in the thymic selection leads to self-reactive T-cells and induction of autoimmune disorders such as MS.[22, 23]

The myelin sheath consists of multiple proteins; MBP and PLP are two of the major component of the myelin sheath, while MOG and Myelin-associated Glycoprotein (MAG) are less abundant.[24, 25] The total myelin proteins consist of only 0.05%-0.1% of MOG;[24, 25] however MOG or MOG epitopes activate T-cell immune responses in Experimental Autoimmune Encephalomyelitis (EAE, animal model of MS) and have also been associated with MS induction.[26, 27] There have been extensive studies of different fragments of MOG as autoimmune triggers.[28-32] The MOG epitopes 1-22, 61-80, 92-106 have been highlighted as target antigens and the 35-55 epitope has been found to induce highly specific antibodies reacting similar to the entire MOG protein.[33, 34] Moreover, T-cell responses to MOG epitopes have been measured through biological assays in MS patients.[29, 30]

The MOG_{35-55} epitope (M^{35}EVGWYR**S**^{42}PFSRVVHLYRNGK^{55}), based on the mouse/rat MOG peptide sequence, is shown as strongly immunogenic in mice leading to the development of chronic EAE.[27, 35] Our group has previously rationally designed and synthesized linear and cyclic peptide analogues of human MOG_{35-55} immunodominant epitope ($hMOG_{35-55}$) with crucial TCR substitutions.[26] These altered peptides have proved to inhibit the clinical manifestation of symptoms of chronic EAE in mice.[26] The substitutions of Arg at positions 41 and 46 by Ala, result in peptide analogues that reduce the severity of MOG-induced EAE clinical symptoms in

C57BL/6 mice when co-administered with mouse/rat MOG_{35-55} peptide at the time of immunization.[26] The observed results justify the importance of Arg at positions 41, 46 for EAE induction.[26]

To the best of our knowledge no conformational study of $hMOG_{35-55}$ epitope in complex with TCR and HLA has been reported. Hence, this is the first attempt to provide a deeper understanding of the structural requirements in the trimolecular complex with $hMOG_{35-55}$ epitope. A detailed analysis of interactions between $hMOG_{35-55}$ and the respective receptors (HLA and TCR) could provide valuable information for rational design of altered peptide ligands (APLs) and non-peptide mimetics with inhibitory activity. Herein, the structural properties of $hMOG_{35-55}$ in three different environments were investigated, through the use of molecular dynamics simulations: i) we looked at the adopted conformations by the peptide in aqueous solution, ii) we carried out MD simulation studies using $hMOG_{35-55}$ in combination with HLA DR2 (DRA, DRB1*1501) receptor and iii) the created trimolecular complex between $hMOG_{35-55}$, HLA DR2 and TCR was explored. The investigation of the interactions between $hMOG_{35-55}$ and the receptors in the trimolecular complex is expected to provide important information on the binding patterns of the hMOG epitope, which can assist researchers in the rational design of novel molecules, focusing on the inhibition of the stimulated encephalitogenic T-cells that are responsible for EAE and MS induction.

2. Methods

The high resolution crystal structure of HLA DR2 (DRA, DRB1*1501) in complex with the MBP_{83-96} antigen (E^{83}NPVVHFFKNIVTP^{96}) and TCR was used for the MD simulations (PDB code: 1ymm).[36] The $hMOG_{35-55}$ epitope (M^{35}EVGWYR**P^{42}**PFSRVVHLYRNGK^{55}), based on the human sequence, used for the simulation studies was constructed using PyMOL.[37] During this process the amino acids (L configuration), comprising the peptide, were placed in sequential order with no initial secondary structure assignment (unfolded conformation). The different systems were subjected to all-atom unrestrained MD simulations in explicit solvent using AMBER14.[38]

2.1 Molecular Dynamics (MD) simulation of $hMOG_{35-55}$

For the construction of the $hMOG_{35-55}$ peptide parameters, the AMBER force field ff14SB[39] has been used. The TIP3P water model[40] was utilized for the solvation of the system and the total charge was neutralized by the addition of three Cl^- ions. Truncated octahedral periodic boundary conditions have been applied to the system with a cutoff distance of 10 Å. The next step involved the minimization, followed by the heating of the system, under constant volume, to 300K for 100ps using the Langevin dynamics temperature scaling.[41] This was followed by equilibration for another 100 ps under constant pressure. Both heating and pressure equilibration were performed using a 10 kcal mol^{-1} $Å^{-2}$ restraint on the solute. The equilibration step under constant pressure was prolonged for a further 200 ps, after removing all restraints. The MD production run was performed under constant pressure and temperature conditions (NPT ensemble) for 100 ns. The temperature was kept constant with the use of the Langevin thermostat (using a collision frequency of 2 ps^{-1}). All bonds involving hydrogen atoms were kept

to their equilibrium distance with the SHAKE algorithm (allowing for a 2 fs time step to be used).[42] The long range electrostatic interactions were calculated with the Particle Mesh Ewald (PME) method.[43]

2.2 Molecular Dynamics (MD) simulation of the hMOG$_{35-55}$ complexed with the HLA DR2 receptor

The positioning of the hMOG$_{35-55}$ epitope inside the HLA DR2 receptor was performed manually using PyMOL.[37] The minimized structure (Section 2.1) of the linear hMOG$_{35-55}$ epitope was superimposed with the crystal structure of the MBP$_{83-96}$ epitope (PDB code: 1ymm).[36] The orientation of hMOG$_{35-55}$ resembles the positioning of the MBP$_{83-96}$ epitope inside the binding pocket of HLA DR2.[36, 44] The residues Tyr^{40}, Pro^{43}, Ser^{45} and Val^{48} of hMOG were placed in the respective pockets (P1, P4, P6 and P9 for HLA DR2), as reported in the literature.[36, 44, 45] In the next step, the residues comprising the TCR were removed along with all crystallographic water molecules. The missing hydrogens were added using the tLeap module in AMBER14.

As with the MD simulation of hMOG$_{35-55}$ in water, the parameters for the receptor were constructed using the AMBER force field ff14SB.[39] The total charge of the system was neutralized with the addition of fourteen Na^+ ions. The TIP3P water model[40] was used in the solvation of the system and truncated octahedral periodic boundary conditions were applied to the system with a cutoff distances of 10 Å. The system was minimized over 5000 steps, followed by the gentle heating to 300K over 100 ps, using the Langevin dynamics temperature scaling (time step 2 fs). The system was further equilibrated under constant pressure for 100 ps. As mentioned in section 2.1, both the heating and equilibration steps were performed using a 10 kcal mol^{-1} Å^{-2} restraint on the solute. A 200 ps equilibration step, under constant pressure, was performed

following the removal of the restraint on the solute. Finally, an MD production run for 40 ns was performed using the NPT ensemble.

2.3 Molecular Dynamics (MD) simulation of TCR-hMOG$_{35-55}$-HLA DR2 complex

For the MD simulation of the hMOG$_{35-55}$ epitope in complex with both TCR and HLA the construction of the system followed the same steps described in section 2.2. The minimized conformation of the linear hMOG$_{35-55}$ epitope (Section 2.1) was superimposed with the crystal structure of HLA DR2/MBP$_{83-96}$/TCR). Thus, the TCR from the crystal structure was positioned over the hMOG$_{35-55}$-HLA DR2 complex. Subsequently, the MBP$_{83-96}$ peptide was removed from the crystal structure along with the water molecules. The preparation of the system and the MD simulation followed the steps mentioned in section 2.2. A total of thirteen Na^+ ions were used to neutralize the system and the solvation of the complex in explicit solvent was done using the TIP3P water model.[40]

A 40 ns MD production run in the created trimolecular complex was performed using AMBER14.[38] Studies in similar biological systems show that the simulation time reported here is adequate for the conformational analysis of the bound epitope.[46-50] The parameters for the proteins and the peptide were constructed using the AMBER ff14SB force field.[39] The next step involved the minimization of the system followed by the heating of the complex to 300 K for 100 ps. Constant pressure equilibration was performed for a total of 300 ps. During the first 100 ps, a 10 kcal mol^{-1} Å^{-2} restraint constant was imposed on the solute, which was then removed for the rest of the equilibration run. The MD production run was attained under isothermal and isobaric conditions and the temperature was kept constant with the use of the Langevin thermostat. The bonds involving hydrogen atoms were kept to their equilibrium

distance with the SHAKE algorithm.[42] The Particle Mesh Ewald (PME) method[43] was implemented for the calculation of the long range electrostatic interactions. Following, the above procedure, we also performed two MD simulations with mutated forms of $hMOG_{35-55}$, namely: $hMOG_{35-55}(Ala^{41})$ and $hMOG_{35-55}(Ala^{41,46})$. In these variants, the Arg was replaced by Ala in position 41 and in positions 41/46, respectively.

2.4 Trajectory and Clustering analysis

The analysis (Rms deviations, atomic fluctuations and clustering calculations) of all the AMBER MD trajectories, was carried out using the cpptraj module[51] of the AMBER14 molecular package. The analysis of the hydrogen bond (HB) interactions was based on geometrical criteria, the limitations imposed were a 3.5 Å cutoff for donor-acceptor distance and a donor-hydrogen-acceptor angle cutoff of 120°. For the clustering analysis of the various MD trajectories, the hierarchical method[52] was used in the grouping process, with the Rms being the distance metric (cutoff 2.0 Å). The representative conformations presented in the paper are snapshots taken from the reference (centroid) simulation frames, used during the clustering analysis by the cpptraj module.

3. Results

3.1 Conformational characteristics of $hMOG_{35-55}$ epitope

The analysis of the MD trajectory for the $hMOG_{35-55}$ in solution revealed that $hMOG_{35-55}$ does not retain an extended form. The different conformations adopted throughout the 100 ns trajectory, showed that the dominant form of the peptide presents two bends (Figure 1a). The particular conformation is displayed on approximately 40% of the simulation time. The bend conformation of the peptide may be partly attributed

to its hydrophobic content (Figure 1b, thicker ribbon). The hydrophobic residues may force the polypeptide chain to seek conformations that decrease their exposure to the solvent. As expected, the small length does not allow the peptide to adopt a more stable secondary structure like α-helix or β-sheet. Instead $hMOG_{35-55}$ remains in a largely unfolded state in aqueous solution, in accordance with experimental observations.[53, 54]

The adoption of a bend conformation by the peptide is further supported by the analysis of the secondary structures of the residues during the MD simulation (Figure S1, in Supporting Information). It is evident that the secondary structure of the peptide does not present a stable conformational profile throughout the MD simulation (Figure S1). Though, it displays certain helical features, such as bends and turns (Figure S1, red and brown colours, respectively). These observations are in close agreement with those reported by Albouz-Abo *et. al* (1997).[53] In the particular paper, Circular Dichroism (CD) data is reported in both the rat and human forms of MOG_{35-55}. The CD experiments show evidence of helical conformations adopted mainly by the rat sequence and to a lesser extent by the human form of MOG in increased concentrations of trifluroethanol.[53] In our theoretical model (Figure 1), the $hMOG_{35-55}$ peptide presents a semi-closed conformation (random coil) as also reported by the study of Albouz-Abo *et. al.* in aqueous solution. The proposed conformation also presents, common features with the closed conformation reported for the rat/mouse MOG_{35-55} peptide by Ntountaniotis, *et. al* (2016, doi.org/10.1080/07391102.2016.1188418)[54] in both DMSO and aqueous solutions. The dominant form of $hMOG_{35-55}$ (Figure 1a, Figure S2), displays two bends in the polypeptide backbone. The first bend is observed between residues Trp^{39}, Tyr^{40} and Arg^{41} (Figure 1a and Figure S1 red colour) and the second in the area defined by residues Val^{48} and Arg^{52} (Figure S1, red colour). The particular conformation of the peptide is defined by the presence of extensive hydrogen bonds

between the different amino acids. The most important interactions are those between residues Glu^{36}-Arg^{41} and Glu^{36}-Phe^{44} (Figure 1a, dark green lines). The hydrogen bond between the backbone carbonyl -O of Glu^{36} and the backbone -NH of Phe^{44} causes the peptide to form a loop, which is further stabilized by the interactions between the side chains of Glu^{36} and Arg^{41} (Figure 1a). This loop appears almost throughout the simulation time as shown by the clustering analysis. Besides the above mentioned dominant form of $hMOG_{35-55}$ (Figure 1c, black), there are two more representative conformations (Figure 1c, blue and green) in the MD simulation. Although both of these conformations retain the loop between residues 35-44, the second bend observed in the dominant form does not appear in these structures. The hydrogen bond between Val^{48} and Arg^{52} (Figure 1a) is absent in these conformations leading to the loss of the second bend in the structure of the peptide.

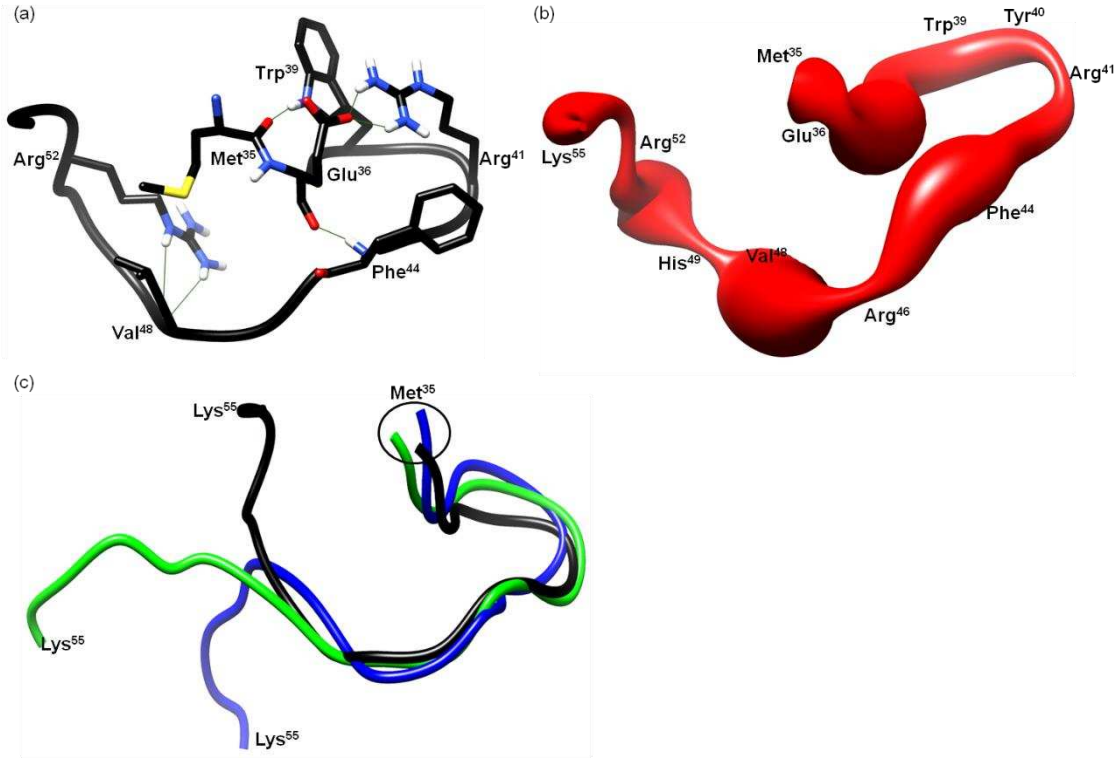

Figure 1: (a) The dominant conformation of the hMOG$_{35-55}$ peptide in water, showing the hydrogen bonds (as green lines) between the residues, (b) schematic representation of the hydrophobic content of the hMOG$_{35-55}$ peptide. The hydrophobicity of each residue is represented by the thickness of the ribbon and (c) superimposition of the three representative conformations of the hMOG$_{35-55}$ peptide in the MD simulation.

3.2 Conformational analysis of hMOG$_{35-55}$-HLA DR2 receptor complex

A visual inspection of all the conformations during the MD simulation was carried out and the amino acids of the hMOG$_{35-55}$ with side chains that were oriented into the HLA DR2 main pockets were recorded (Figure S3). The conformational analysis of the hMOG$_{35-55}$-HLA DR2 complex showed that the peptide occupies pockets 1, 4, 6 and 9 of the receptor (Figure S3). These four pockets are the same areas occupied by the MBP$_{83-96}$ epitope (Figure 2). The clustering analysis in the MD

production run of $hMOG_{35-55}$-HLA DR2 complex revealed that the dominant conformation of the peptide is the one depicted in Figures 2 and S3. In fact, the particular conformation is found to be present for approximately 70% of the simulation time. This observation may suggest that the $hMOG_{35-55}$ epitope favours a particular conformation when bound to HLA DR2 and retains this structure during most of the simulation time. The Rms deviations recorded during the MD simulation, show that both $hMOG_{35-55}$ and the HLA receptor retain a stable configuration throughout the MD simulation (Figure 3a and 3b, blue), with respect to their initial configuration.

A more detailed examination showed that in pockets 1, 6 and 9, the residues interacting with the HLA DR2 receptor are similar in nature to those of the MBP_{83-96} epitope occupying the same space in the receptor (Figure 3). For instance, Tyr^{40} ($hMOG_{35-55}$) and Val^{87} (MBP_{83-96}) have both hydrophobic side chains and are oriented towards a buried area of the HLA receptor in pocket P1 (Figure 2). The specific area of the receptor is rich in hydrophobic residues, such as Phe^{24}, Phe^{26}, Ile^{31}, Phe^{54} and Val^{85} (Figure 2, red surface colour). Moreover, the bulkier side chain of Tyr^{40} ($hMOG_{35-55}$) is buried deeper in the particular pocket of HLA and may enhance the hydrophobic interactions between the epitope and the receptor, compared to MBP_{83-96}. A similar trend is observed in the P6 pocket of HLA with the presence of Ser^{45} ($hMOG_{35-55}$) and Asn^{92} (MBP_{83-96}), which both present polar side chains. The -OH group from Ser^{45} ($hMOG_{35-55}$) interacts with neighbouring residues such as Glu^{31}, Asn^{62} and Asp^{66} of the HLA. Likewise, the amide side chain of Asn^{92} (MBP_{83-96}) interacts with the same amino acids of the receptor in the P6 pocket. Finally, in P9 pocket both $hMOG_{35-55}$ and MBP_{83-96} have in the same position (48 and 94, respectively) a Val residue, surrounded by amino acids Val^{65} and Ala^{68} of the receptor (Figure 2). The only difference between the two epitopes is focused in the P4 pocket of HLA DR2. In $hMOG_{35-55}$ there is Pro^{43} in

the P4 pocket of HLA while MBP_{83-96} has a hydrophobic residue (Phe^{90}) at the same position. The P4 pocket of the receptor includes residues with polar side chains, thus the smaller and restricted side chain of Pro may induce conformational changes in the residues surrounding Pro^{43} that may lead to a better positioning inside the P4 pocket of the HLA receptor.[55]

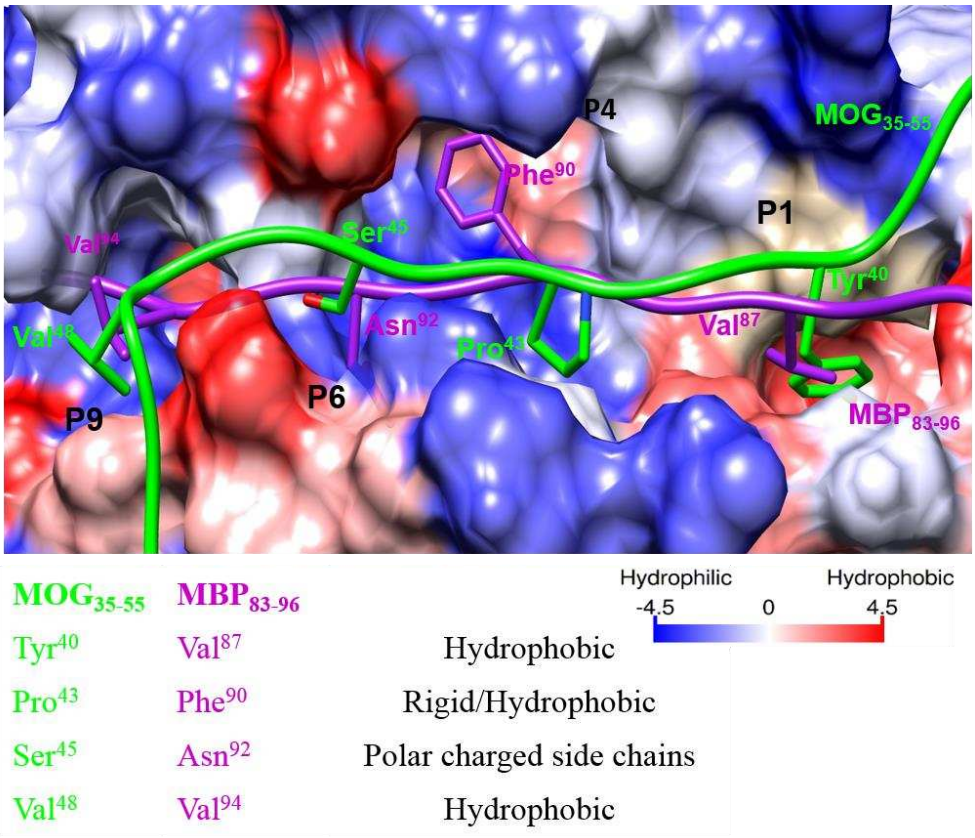

Figure 2: The binding cavity, depicted as surface, of HLA DR2 shows the pockets P1, P4, P6 and P9 in the dominant representative conformation of the HLA DR2 -$hMOG_{35-55}$ complex. The $hMOG_{35-55}$ (green) epitope is superimposed with the crystal structure of MBP_{83-96} (purple) taken from the crystal structure 1ymm. The peptides' backbone is represented as ribbon and the side chains of the residues are outlined as sticks. The surface of the receptor is coloured according to the Kyte-Doolittle hydrophobic index.

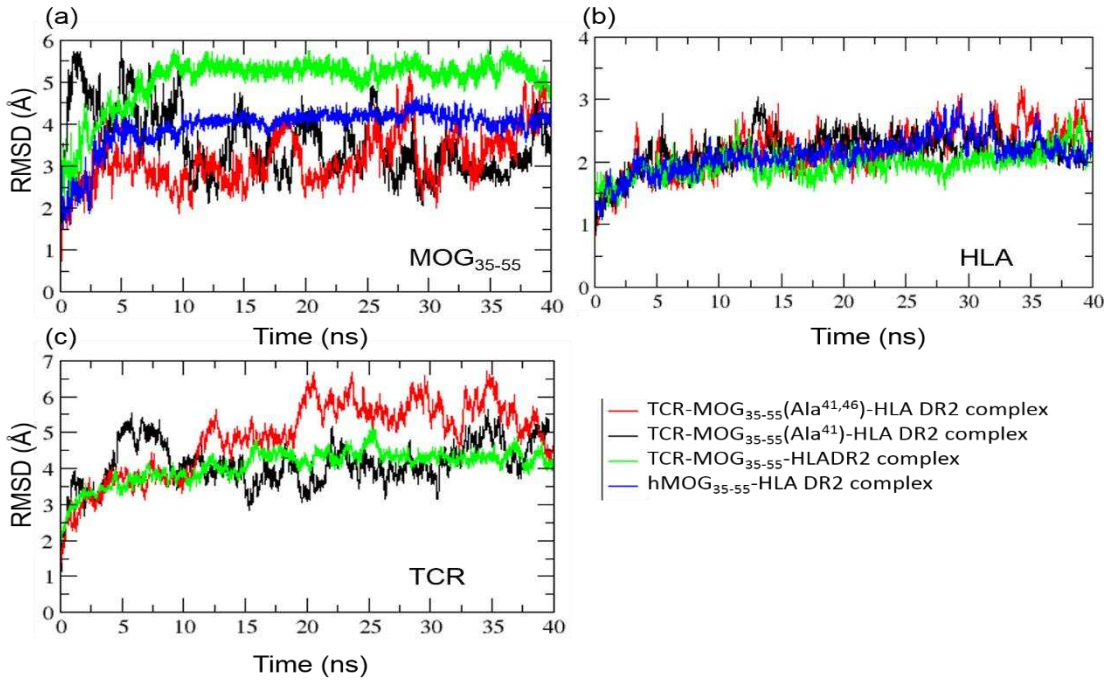

Figure 3: RMS deviations of the backbone Cα atoms in all MD simulation runs in comparison to their starting configurations for (a) $hMOG_{35-55}$, (b) HLA DR2 receptor and (c) TCR.

3.2.1 Hydrogen bond interactions in $hMOG_{35-55}$-HLA DR2 receptor complex

A detailed analysis of the hydrogen bonds (HBs), between the amino acids of $hMOG_{35-55}$ and the HLA DR2 receptor, was carried out and the results are presented in Table 1. An important feature observed in the analysis of the MD simulation is the lack of water mediated hydrogen bonds between the peptide and the receptor. The binding cavity includes residues with bulky side chains such as Asn^{69}, Gln^{71}, Arg^{76}, His^{81} and Asn^{82} in HLA (Table 1), that may prevent water molecules to move between receptor and epitope residues and consequently interact with either.

Table 1: Residues in HLA DR2 receptor that are involved in HBs with those of the $hMOG_{35-55}$ epitope, as recorded in all the MD simulations.

Peptide sequence [a]	MD simulations[b]			
		TCR-$hMOG_{35-55}$-HLA complexes		
	$hMOG_{35-55}$-HLA[c]	$hMOG_{35-55}$	$hMOG_{35-55}$ (Ala^{41})	$hMOG_{35-55}$ ($Ala^{41,46}$)
Met^{35}	–	–	–	Glu^{87}
Glu^{36}	–	–	–	Arg^{80},Glu^{87}
Val^{37}	Arg^{80}	–	–	–
Trp^{39}	Arg^{80}	Thr^{77},Arg^{80}	Arg^{80}	–
Tyr^{40}	His^{81}	His^{81},Asn^{82}	-	Glu^{55}
Arg^{41}	Gln^{70}	Glu^{55}	His^{81}	Tyr^{78}
Pro^{43}	Asn^{62}	–	–	–
Phe^{44}	–	Gln^{70}	Gln^{70}	Gln^{70}
Ser^{45}	Asp^{66},Asn^{62}	–	Asn^{62}	Asn^{62},Arg^{13}
Arg^{46}	–	Asp^{66}	Gln^{64}	–
Val^{47}	–	-	–	Asn^{69}
Val^{48}	–	-	Gln^{64}	–
His^{49}	–	Ala^{61}	Asp^{66}	Asn^{69}
Leu^{50}	–	–	–	Tyr^{60}
Tyr^{51}	Ala^{64}	–	Pro^{56}	–
Arg^{52}	Lys^{67}	–	–	Asp^{57}
Lys^{55}	Gln^{18}	–	–	–

[a] Only the residues involved in hydrogen bonds are presented here

[b] For detailed information on hydrogen bonds see Table S1 in Supporting Information.

[c] Only HBs with occurrence of more than 20% of the simulation time are presented here.

As observed in Table 1, $hMOG_{35-55}$ creates an extensive hydrogen bond network with the HLA receptor. In pocket P1 of the HLA DR2, Tyr^{40} interacts with His^{81} from HLA anchoring the peptide in such a way to facilitate the interactions of its neighbouring residues (namely Trp^{39}, Arg^{41} and Pro^{43}). In fact Trp^{39} is involved in interactions with Arg^{80} in P1 pocket as well as Ser^{53} which is located in proximity to P1 pocket. Moreover, Arg^{41} due to its polar side chain, creates hydrogen bonds with three different amino acids of HLA (Gln^{70}, Asp^{76} and Thr^{77}, Table 1) that are located in the P4 pocket and its vicinity, although such interactions are not appearing throughout the simulation time. This may be explained by the fact that the side chain of Arg^{41} is positioned towards the external area of the HLA receptor in a solvent exposed environment and may lead to extensive interactions with the TCR. Finally, Pro^{43} is

interacting with Asn^{62}, located in the area between pockets P4 and P6 of the HLA, with the particular interaction being present throughout most of the simulation time. The particular HB interaction may enhance the HBs created between Arg^{41} and the receptor. Another residue of $hMOG_{35-55}$, implicated in HB formation is Ser^{45}, which forms extensive HBs with Asn^{62} and Asp^{66} in P6 of the HLA receptor. Even residues such as Arg^{52} and Lys^{55} of the peptide, despite being positioned outside the binding areas P1, P4, P6 and P9 are interacting with residues of the HLA (Lys^{67} and Gln^{18}, Gly^{20}, respectively). These extensive interactions with the receptor may increase the binding affinity of the $hMOG_{35-55}$.

As mentioned in section 3.1, $hMOG_{35-55}$ adopts a bend conformation due to the presence of HB formed between residues such as Glu^{36} and Phe^{44} (Figure 1). When bound to the HLA DR2 receptor, this conformational feature is not retained (Figure 2) which is expected, since the interactions between the epitope and the residues of the receptor may lead to a conformational rearrangement of the epitope in order to enhance its binding. The bend aspect of the $hMOG_{35-55}$ peptide is an essential feature, because it allows the epitope to reach inside the receptor. Thus, residues such as Tyr^{40} and Pro^{43} may interact with residues in different pockets (P1 and P4, respectively) and create a more extensive HB network with the HLA DR2 molecule.

3.3 Conformational analysis of the trimolecular complex (TCR-$hMOG_{35-55}$-HLA DR2)

As discussed in the Methods section (Section 2.3), the positioning of the $hMOG_{35-55}$ epitope in the trimolecular complex was carried out *via* the superimposition of the epitope with the crystal structure of the MBP_{83-96} peptide. Thus, the amino acids of

$hMOG_{35-55}$ and MBP_{83-96} occupy similar pockets inside the TCR and HLA DR2 receptors. Furthermore, as reported in Section 3.2, $hMOG_{35-55}$ retains its initial positioning in the HLA DR2 pockets 1, 4, 6 and 9 throughout the simulation. In that respect, residues such as Arg^{41} and mainly Arg^{46} of the peptide are facing towards the solvent when bound to HLA allowing the peptide to create enhanced interactions with the TCR during the antigen recognition process. This can be partially explained by the relative stable conformations observed in the trimolecular complex in the MD simulation. The Rms values for $hMOG_{35-55}$ and the two receptors (HLA and TCR) after the first 5 ns of the simulation, remain relatively stable throughout the MD run (Figure 3, green). This observation is in accordance with the conformational changes in the $hMOG_{35-55}$-HLA DR2 complex. The conformational changes of the HLA receptor are similar in the trimolecular and $hMOG_{35-55}$-HLA DR2 complexes (Figure 3b, green and blue), as well as in the $hMOG_{35-55}$ epitope (Figure 3a, green and blue). The difference, compared to the starting configuration, for the peptide in the two systems can be attributed to the interactions arising between $hMOG_{35-55}$ and both receptors in the case of the trimolecular complex (Figure 3a).

3.3.1 Clustering analysis of the trimolecular complex (TCR-$hMOG_{35-55}$-HLA DR2)

The clustering analysis showed that there are four representative clusters throughout the simulation (Figure 4a). The different conformations of $hMOG_{35-55}$ in their majority are exemplified by the bend conformation (Figure 4a, red). The particular conformation is appearing at 67% of the frames in our simulation. The other three clusters are present for a small percent of the simulation each, and are mostly appearing during the first 5 ns, suggesting that the peptide prefers the bend conformation that is

appearing on Pro[42,43], in the presence of TCR and HLA. The aforementioned conformation may play a role in the orientation of hMOG$_{35-55}$ in the binding pocket of TCR. One such example is the positioning of Arg[41] inside pockets P2 and P3 of TCR (Figure 4b) that may lead to enhanced interactions with the TCR. Moreover, it may orient other residues of hMOG$_{35-55}$ in such a way so as to be correctly placed in the binding cavity of TCR. The orientation of the peptide in the TCR does not affect only the interactions between hMOG$_{35-55}$ and TCR, but also the interactions with the HLA receptor.

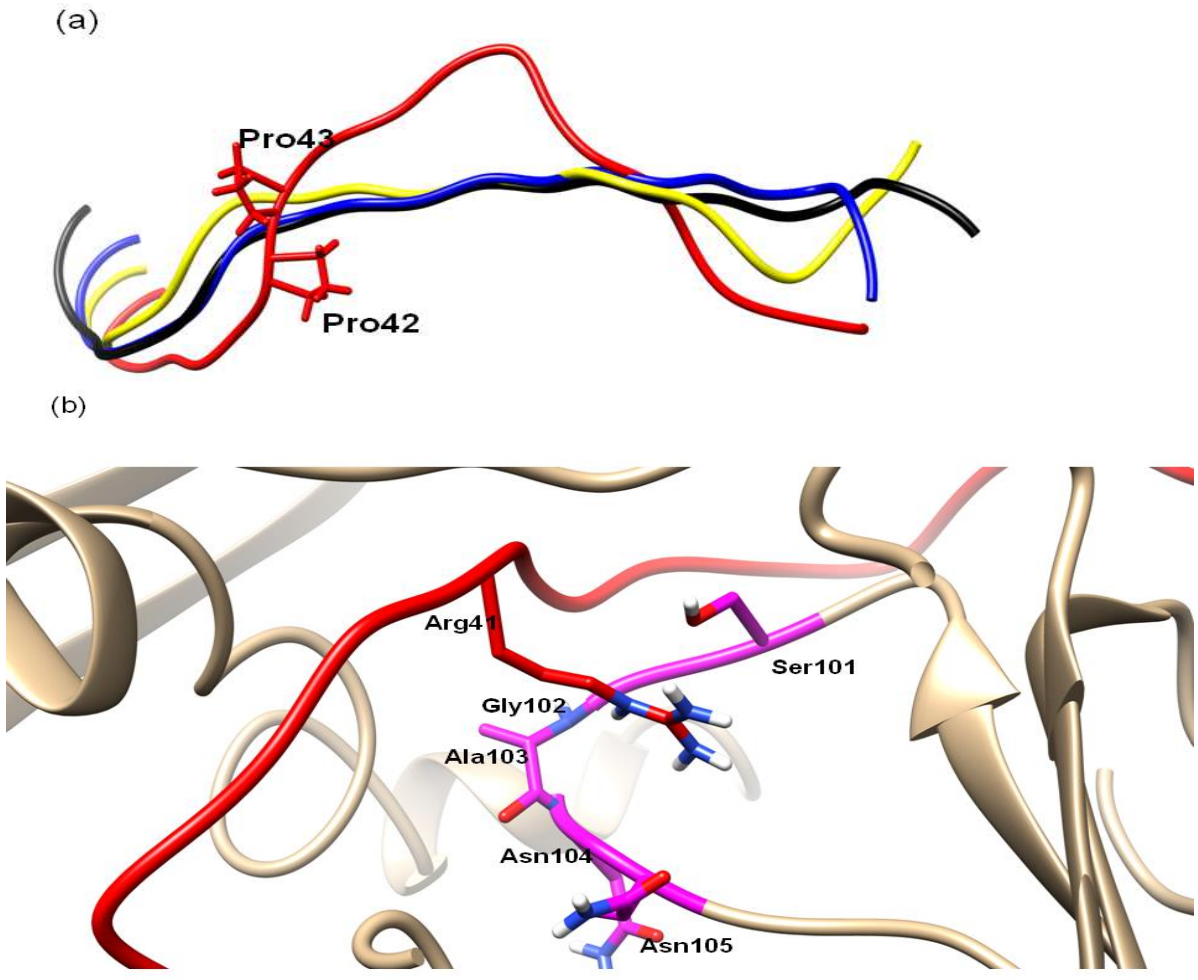

Figure 4: (a) Representative structures of the 4 clusters generated from the MD simulation of the trimolecular complex (TCR-hMOG$_{35-55}$-HLA DR2). In red is the representative conformation of the most dominant cluster (67%) during the simulation.

(b) The position of Arg^{41} (dominant cluster) in the TCR pockets P2, P3 and the proximity to residues 101-105 allow the Arg to form extensive HBs, as reported in Table 2.

3.3.2 Hydrogen bond interactions in the trimolecular complex (TCR–$hMOG_{35-55}$–HLA DR2)

It was observed in the $hMOG_{35-55}$-HLA DR2 complex that Tyr^{40} ($hMOG_{35-55}$) is positioned similarly to Val^{89} (MBP_{83-96}) and also creates HBs with the same amino acid -namely His^{81}- of HLA in the trimolecular complex (Table 1). Similarly, in the trimolecular complex, Trp^{39} ($hMOG_{35-55}$) participates in HB formation with residues (Arg^{80}, Thr^{77}) inside pocket P1 of the HLA DR2 receptor (Table 1). The interactions of $hMOG_{35-55}$ with the TCR are reported in Table 2. In general, $hMOG_{35-55}$ retains similar HB interactions when bound either to HLA or TCR and HLA together (Table 1) and the most important residues of the epitope are the two Arg in positions 41 and 46

Table 2: TCR residues that interact with residues of the $hMOG_{35-55}$ epitope for the formation of respective HBs, as recorded in all the MD simulations.

	TCR-$hMOG_{35-55}$-HLA MD simulations[b]		
Peptide sequence[a]	$hMOG_{35-55}$	$hMOG_{35-55}(Ala^{41})$	$hMOG_{35-55}(Ala^{41,46})$
Met^{35}	Thr^{94}	–	–
Glu^{36}	Ser^{28}	–	Ser^{28}
Gly^{38}	Ser^{95}	Ser^{95}	Ser^{95}
Trp^{39}	–	–	Ala^{103},Gly^{96}
Tyr^{40}	Tyr^{98}	Tyr^{98}	–
Arg^{41}	Gly^{102},Asn^{104}	–	–
Ser^{45}	–	Thr^{100}	–
Arg^{46}	Asp^{98},Thr^{100}, Glu^{106}	Asp^{98},Thr^{100}, Gly^{106}	–
Arg^{52}	Ser^{25}	–	–
Asn^{53}	Gln^{29},Thr^{75}	–	–
Gly^{54}	–	–	–
Lys^{55}	Arg^{24}	–	–

[a] Only the residues involved in hydrogen bonds are presented here

[b] For detailed information on hydrogen bonds see Table S2 in Supporting Information.

It has been theorised that Pro^{42} in $hMOG_{35-55}$ plays a crucial role in the binding of the peptide to the TCR. The rigid region around Pro^{42}-Pro^{43} (Figure 4a) seems to create a bend in the peptide. This structural feature allows the peptide to bend in a way that assists the interactions between Arg^{41} of the peptide and the TCR. In fact, Arg^{41} seems to reach easier into the pocket P3 of the TCR, in the presence of this bend. This conformational change may be the reason for the enhanced HB interactions of Arg^{41} with residues Gly^{102} and Asn^{104} in TCR. Also, it may lead to the HB formation between Arg^{46} and residues Asp^{98}, Thr^{100} and Glu^{106} of the TCR. These interactions are present in the majority of the frames of the MD trajectory. Arg^{46} is positioned in the middle of $hMOG_{35-55}$; hence the HBs formed with the TCR may further anchor the peptide firmly on the space between the two receptors. In this context, residues such as Asn^{53} that does not interact with any of the residues in the HLA receptor forms hydrogen bonds with Gln^{29} and Thr^{75} of the TCR (Table 2). These interactions are also present for most of the simulation time.

3.3.3 Conformation characteristics of mutated $hMOG_{35-55}(Ala^{41})$ and $hMOG_{35-55}(Ala^{41,46})$ analogues

The conformational analysis of the $hMOG_{35-55}(Ala^{41})$ and $hMOG_{35-55}(Ala^{41,46})$ analogues, revealed that the conformational changes in the peptide are more evident in the two variations of $hMOG_{35-55}$ compared to the $hMOG_{35-55}$ epitope (Figure 3a, red and black). The mutation in positions 41 and 46 of the $hMOG_{35-55}$, affects the conformations of the peptide in the trimolecular complex. The substitution of Arg with Ala in both cases leads to loss of interactions between the peptide and the two receptors (HLA, TCR). The mutations and the subsequent change in the interactions formed by the peptide may explain the greater fluctuations with respect to the initial conformation

of the RMS values in Figure 3a (red and blue) over time compared to the $hMOG_{35-55}$ epitope (Figure 3a, green). Moreover, the clustering analysis performed in the two variants of the $hMOG_{35-55}$ epitope, showed that there is a dominant conformation for the peptides inside the trimolecular complex (approximately 72% of the simulation time) as presented in Figure 5.

The analysis of the hydrogen bond interactions between the two mutated analogues of $hMOG_{35-55}$, showed a loss of interactions with the receptors mainly with TCR (Table 2). As expected the particular loss is centered on the positions with the mutated amino acids (positions 41 and 46). The replacement of Arg by Ala causes the loss of the HBs observed in $hMOG_{35-55}$ (Tables 2), that could be attributed to the increased polarity of Arg due to the guanidino group that can create an extensive interaction pattern. On the other hand, Ala bears a less bulky group, as a side chain, with no potential for creating hydrogen bonds. This mutation may cause indivertibly, conformational changes in the positioning of the peptide inside the cavity of the two receptors. As presented in Figure 5 (red), the dominant conformation of the wt–$hMOG_{35-55}$ peptide is more bend when compared to the representative conformations adopted during the MD simulations by $hMOG_{35-55}(Ala^{41})$ (Figure 5, green) and $hMOG_{35-55}(Ala^{41,46})$ (Figure 5, yellow). The Arg in positions 41 and 46 are found on either side of a loop in the TCR binding site with polar residues such as Asp^{98}, Ser^{101} and Asn^{104}. These polar residues interact with Arg in the $hMOG_{35-55}$ epitope and assist to anchor the peptide in the TCR receptor. These interactions are not present on the $hMOG_{35-55}(Ala^{41})$ and $hMOG_{35-55}(Ala^{41,46})$ variants.

Additionally, a significant aspect observed in the three different MD simulations of the trimolecular complex (TCR-$hMOG_{35-55}$-HLA DR2 receptor) is the retention of

the interactions of Phe at position 44 of the $hMOG_{35-55}$ epitope. In both variants of $hMOG_{35-55}$ and in the $hMOG_{35-55}$, the particular residue forms hydrogen bonds with Gln^{70} in the HLA receptor (Table 1) that are present throughout the MD simulation.

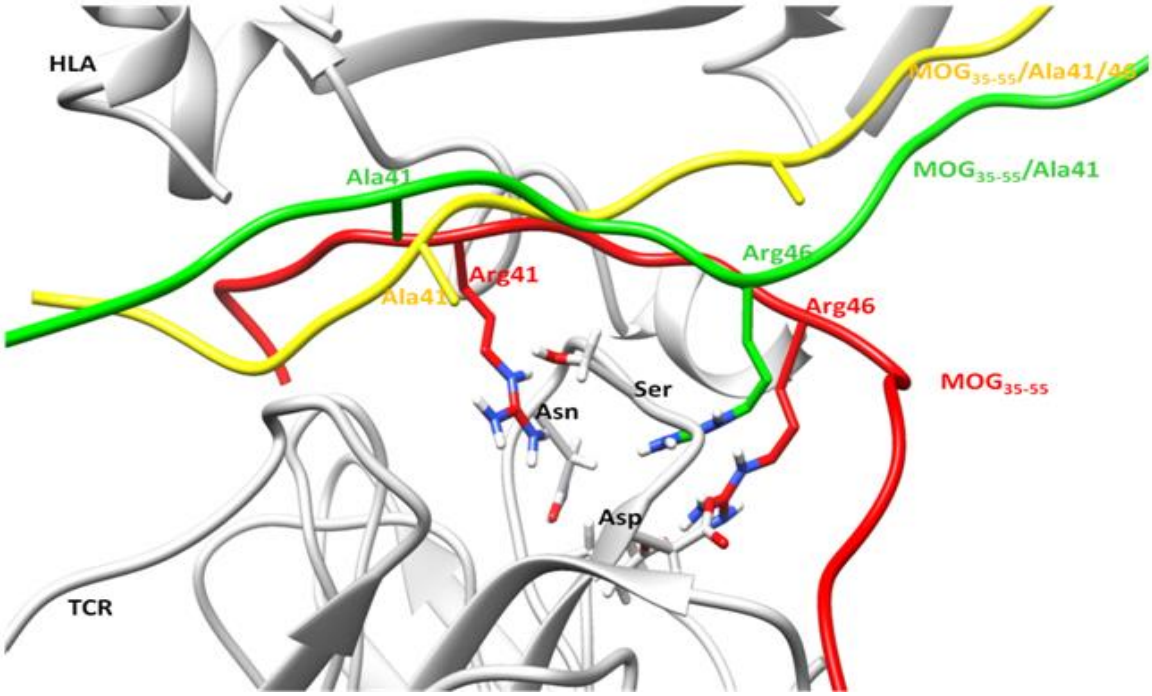

Figure 5: The dominant representative conformations of the $hMOG_{35-55}$ (red) and the two variants $hMOG_{35-55}(Ala^{41})$ (green) and $hMOG_{35-55}(Ala^{41,46})$ (yellow) at the interface between the HLA receptor (top) and TCR (bottom). The residues at positions 41 and 46 are presented as sticks while the rest of the proteins are presented as ribbon.

4. Discussion

The theoretical analysis based on the MD simulations, shows that $hMOG_{35-55}$ can be an important activator of T-cells. The conformational analysis inside the HLA receptor and in the trimolecular complex revealed similar positioning with the MBP_{83-96} peptide, suggesting a comparable mode of interaction between the two epitopes and the two receptors. In regard to the interactions between the epitopes and the HLA-DR2 receptor, we observe that the residues involved in HBs have similar chemical properties (Figure 2). These similarities (hydrophobic nature, charged side chains) may provide valuable information regarding the type of interactions between the different epitopes and the receptor. Thus, it is possible to cluster the interactions of the epitopes in groups and identify common patterns. The comparison of these interactions between the $hMOG_{35-55}$ epitope and the HLA are comparable to those of MBP_{83-96} (Figure 2), nevertheless these two antigens exhibit a sequence similarity of only 14%. This may be partially explained by the fact that the residues interacting with the receptor have similar side chains (Figure 2).

The majority of HBs between the $hMOG_{35-55}$ epitope and the HLA DR2 receptor stems mainly from residues Trp^{39} and Arg^{41}. The same Arg also presents a high number of interactions with the TCR, suggesting that the particular residue plays a critical role in antigen identification by T-cells. It can also be deduced that the approach of TCR towards the peptide/HLA DR2 receptor complex leads to the increase of the HBs inside the newly formed trimolecular complex. Subsequently, this might indicate that the antigen binding affinity is amplified once it is placed between the two receptors.

We concluded that key residues that enable the interactions between $hMOG_{35-55}$ and the TCR are Arg^{41} and Arg^{46}. Arg at positions 41 and 46 of the peptide create an extensive HB network with both receptors. The substitution of Arg, at positions 41 and

46 of the epitope, with Ala leads to changes in the interactions of the peptide. Ala, in contrast to Arg, has a very small, non-polar side chain group that subsequently may affect the potential of the peptide to interact with TCR, since the particular position is solvent exposed and thus favours the presence of hydrophilic residues. As observed with the two variants of $hMOG_{35-55}$ [$hMOG_{35-55}(Ala^{41})$ and $hMOG_{35-55}(Ala^{41,46})$], the mutation of Arg to Ala leads to loss of interactions between the TCR and $hMOG_{35-55}$ (Table 2), while retaining the same pattern of HBs and binding affinity towards the HLA receptor (Table 1). In both the $hMOG_{35-55}$ and its mutations, the interactions between Phe^{44} and the HLA receptor are identical in nature.

5. Conclusion

The peptide variants [$hMOG_{35-55}(Ala^{41})$ and $hMOG_{35-55}(Ala^{41,46})$] have proved to act as inhibitors of EAE, which is the animal model for MS.[26] The information compiled during our studies confirms that the mutation of key residues in $hMOG_{35-55}$ leads to competitive binding to the HLA receptor and loss of key interactions with the TCR, thus preventing the formation of the trimolecular complex. This report provides a comprehensive theory regarding the interactions and conformational changes observed in the formation of the trimolecular complex (TCR-$hMOG_{35-55}$-HLA DR2 receptor) and highlights key interactions of the $hMOG_{35-55}$ epitope.

Acknowledgements:

This work is financially supported by the "Cooperation" Program 09SYN21-609 and by "Cooperation Greece-Israel Program" ISR-3148 O.P. Competitiveness & Entrepreneurship (EPAN II), ROP Macedonia- Thrace, ROP Crete and Aegean Islands,

ROP Thessaly- Mainland Greece- Epirus, ROP Attica. We also thank FICYT and the European Union (7th WP) for a Marie Curie CLARIN-cofund fellowship to CS.

Conflicts of Interest

The authors declare no conflict of interest.

References

[1] Steinman, L. Multiple sclerosis: a coordinated immunological attack against myelin in the central nervous system. *Cell*. (1996), *85*, 299-302.

[2] Sospedra, M., Martin, R. Immunology of multiple sclerosis. *Annu Rev Immunol*. (2005), *23*, 683-747.

[3] Smith, K.J., Pyrdol, J., Gauthier, L., Wiley, D.C., Wucherpfennig, K.W. Crystal structure of HLA-DR2 (DRA*0101, DRB1*1501) complexed with a peptide from human myelin basic protein. *J Exp Med*. (1998), *188*, 1511-1520.

[4] Shahrizaila, N., Yuki, N. Guillain-barre syndrome animal model: the first proof of molecular mimicry in human autoimmune disorder. *J. Biomed Biotechnol*. (2011), *2011*, 829129.

[5] Moise, L., Beseme, S., Tassone, R., Liu, R., Kibria, F., Terry, F., *et al.* T Cell Epitope Redundancy: Cross-conservation of the TCR face between Pathogens and Self and its Implications for Vaccines and Auto-immunity. *Expert Rev Vaccines*. (2016), 15, 607-617.

[6] Compston, A., Coles, A. Multiple sclerosis. *Lancet*. (2002), *359*, 1221-1231.

[7] Davis, M.M., Boniface, J.J., Reich, Z., Lyons, D., Hampl, J., Arden, B., *et al.* Ligand recognition by alpha beta T cell receptors. *Annu Rev Immunol*. (1998), *16*, 523-544.

[8] Wootla, B., Eriguchi, M., Rodriguez, M. Is multiple sclerosis an autoimmune disease? *Autoimmune Dis*. (2012), *2012*, 969657.

[9] Hare, B.J., Wyss, D.F., Osburne, M.S., Kern, P.S., Reinherz, E.L., Wagner, G. Structure, specificity and CDR mobility of a class II restricted single-chain T-cell receptor. *Nat Struct Biol*. (1999), *6*, 574-581.

[10] Rudolph, M.G., Wilson, I.A. The specificity of TCR/pMHC interaction. *Curr Opin Immunol*. (2002), *14*, 52-65.

[11] Rudolph, M.G., Stanfield, R.L., Wilson, I.A. How TCRs bind MHCs, peptides, and coreceptors. *Annu Rev Immunol*. (2006), *24*, 419-466.

[12] Lassmann, H. Axonal and neuronal pathology in multiple sclerosis: what have we learnt from animal models. *Exp Neurol*. (2010), *225*, 2-8.

[13] Reuter, E., Gollan, R., Grohmann, N., Paterka, M., Salmon, H., Birkenstock, J., *et al.* Cross-recognition of a myelin peptide by CD8+ T cells in the CNS is not sufficient to promote neuronal damage. *J Neurosci*. (2015), *35*, 4837-4850.

[14] Madden, D.R. The three-dimensional structure of peptide-MHC complexes. *Annu Rev Immunol*. (1995), *13*, 587-622.

[15] Adams, E.J., Luoma, A.M. The adaptable major histocompatibility complex (MHC) fold: structure and function of nonclassical and MHC class I-like molecules. *Annu Rev Immunol*. (2013), *31*, 529-561.

[16] Feng, Y., van der Veeken, J., Shugay, M., Putintseva, E.V., Osmanbeyoglu, H.U., Dikiy, S., *et al.* A mechanism for expansion of regulatory T-cell repertoire and its role in self-tolerance. *Nature*. (2015), *528*, 132-136.

[17] Yang, X., Gao, M., Chen, G., Pierce, B.G., Lu, J., Weng, N.P., *et al.* Structural Basis for Clonal Diversity of the Public T Cell Response to a Dominant Human Cytomegalovirus Epitope. *J Biol Chem*. (2015), *290*, 29106-29119.

[18] Arstila, T.P., Casrouge, A., Baron, V., Even, J., Kanellopoulos, J., Kourilsky, P. A direct estimate of the human alphabeta T cell receptor diversity. *Science*. (1999), *286*, 958-961.

[19] Hesnard, L., Legoux, F., Gautreau, L., Moyon, M., Baron, O., Devilder, M.C., *et al.* Role of the MHC restriction during maturation of antigen-specific human T cells in the thymus. *Eur J Immunol*. (2016), 46, 560-569.

[20] Buckley, M.W., Trampont, P.C., Arandjelovic, S., Fond, A.M., Juncadella, I.J., Ravichandran, K.S. ShcA regulates late stages of T cell development and peripheral CD4+ T cell numbers. *J Immunol*. (2015), *194*, 1665-1676.

[21] Gianchecchi, E., Delfino, D.V., Fierabracci, A. Recent insights on the putative role of autophagy in autoimmune diseases. *Autoimmun Rev*. (2014), *13*, 231-241.

[22] Chang, H.D., Radbruch, A. Targeting pathogenic T helper cell memory. *Ann Rheum Dis*. (2011), *70 Suppl 1*, i85-87.

[23] Lessard, C.J., Ice, J.A., Adrianto, I., Wiley, G.B., Kelly, J.A., Gaffney, P.M., *et al.* The genomics of autoimmune disease in the era of genome-wide association studies and beyond. *Autoimmun Rev*. (2012), *11*, 267-275.

[24] Jahn, O., Tenzer, S., Werner, H.B. Myelin proteomics: molecular anatomy of an insulating sheath. *Mol Neurobiol*. (2009), *40*, 55-72.

[25] Patzig, J., Jahn, O., Tenzer, S., Wichert, S.P., de Monasterio-Schrader, P., Rosfa, S., *et al.* Quantitative and integrative proteome analysis of peripheral nerve myelin identifies novel myelin proteins and candidate neuropathy loci. *J Neurosci*. (2011), *31*, 16369-16386.

[26] Tselios, T., Aggelidakis, M., Tapeinou, A., Tseveleki, V., Kanistras, I., Gatos, D., *et al.* Rational design and synthesis of altered peptide ligands based on human myelin

oligodendrocyte glycoprotein 35-55 epitope: inhibition of chronic experimental autoimmune encephalomyelitis in mice. *Molecules*. (2014), *19*, 17968-17984.

[27] Delarasse, C., Smith, P., Baker, D., Amor, S. Novel pathogenic epitopes of myelin oligodendrocyte glycoprotein induce experimental autoimmune encephalomyelitis in C57BL/6 mice. *Immunology*. (2013), *140*, 456-464.

[28] Kerlero de Rosbo, N., Milo, R., Lees, M.B., Burger, D., Bernard, C.C., Ben-Nun, A. Reactivity to myelin antigens in multiple sclerosis. Peripheral blood lymphocytes respond predominantly to myelin oligodendrocyte glycoprotein. *J Clin Invest*. (1993), *92*, 2602-2608.

[29] Varrin-Doyer, M., Shetty, A., Spencer, C.M., Schulze-Topphoff, U., Weber, M.S., Bernard, C.C., *et al.* MOG transmembrane and cytoplasmic domains contain highly stimulatory T-cell epitopes in MS. *Neurology(R) neuroimmunology & neuroinflammation*. (2014), *1*, e20.

[30] Shetty, A., Gupta, S.G., Varrin-Doyer, M., Weber, M.S., Prod'homme, T., Molnarfi, N., *et al.* Immunodominant T-cell epitopes of MOG reside in its transmembrane and cytoplasmic domains in EAE. *Neurology(R) neuroimmunology & neuroinflammation*. (2014), *1*, e22.

[31] Linares, D., Mana, P., Goodyear, M., Chow, A.M., Clavarino, C., Huntington, N.D., *et al.* The magnitude and encephalogenic potential of autoimmune response to MOG is enhanced in MOG deficient mice. *J Autoimmun*. (2003), *21*, 339-351.

[32] Krishnamoorthy, G., Saxena, A., Mars, L.T., Domingues, H.S., Mentele, R., Ben-Nun, A., *et al.* Myelin-specific T cells also recognize neuronal autoantigen in a transgenic mouse model of multiple sclerosis. *Nat Med*. (2009), *15*, 626-632.

[33] Pacini, G., Ieronymaki, M., Nuti, F., Sabatino, G., Larregola, M., Aharoni, R., *et al.* Epitope mapping of anti-myelin oligodendrocyte glycoprotein (MOG) antibodies in

a mouse model of multiple sclerosis: microwave-assisted synthesis of the peptide antigens and ELISA screening. *J Pept Sci*. (2016), 22, 52-58.

[34] Mony, J.T., Khorooshi, R., Owens, T. MOG extracellular domain (p1-125) triggers elevated frequency of CXCR3+ CD4+ Th1 cells in the CNS of mice and induces greater incidence of severe EAE. *Mult Scler*. (2014), *20*, 1312-1321.

[35] Bittner, S., Afzali, A.M., Wiendl, H., Meuth, S.G. Myelin oligodendrocyte glycoprotein (MOG35-55) induced experimental autoimmune encephalomyelitis (EAE) in C57BL/6 mice. *J Vis Exp : JoVE*. (2014).

[36] Hahn, M., Nicholson, M.J., Pyrdol, J., Wucherpfennig, K.W. Unconventional topology of self peptide-major histocompatibility complex binding by a human autoimmune T cell receptor. *Nat Immunol*. (2005), *6*, 490-496.

[37] Pokorna, J., Machala, L., Rezacova, P., Konvalinka, J. Current and Novel Inhibitors of HIV Protease. *Viruses*. (2009), *1*, 1209-1239.

[38] Case, D.A., Berryman, J.T., Betz, R.M., Cerruti, D.S., Cheatham, I., T. E., Darden, T.A., *et al. AMBER 2015, University of California, San Francisco, CA*. (2015).

[39] Maier, J.A., Martinez, C., Kasavajhala, K., Wickstrom, L., Hauser, K.E., Simmerling, C. ff14SB: Improving the Accuracy of Protein Side Chain and Backbone Parameters from ff99SB. *J Chem Theory Comput*. (2015), *11*, 3696-3713.

[40] Jorgensen, W.L., Chandrasekhar, J., Madura, J.D., Impey, R.W., Klein, M.L. Comparison of Simple Potential Functions for Simulating Liquid Water. *J-Chem Phys*. (1983), *79*, 926-935.

[41] Izaguirre, J.A., Catarello, D.P., Wozniak, J.M., Skeel, R.D. Langevin stabilization of molecular dynamics. *J-Chem Phys*. (2001), *114*, 2090-2098.

[42] Ryckaert, J.P., Ciccotti, G., Berendsen, H.J.C. Numerical integration of the Cartesian Equations of Motion of a System with Constraints: Molecular Dynamics of n-Alkanes. *J Comp Phys*. (1977), *23*, 327-341.

[43] Darden, T., York, D., Pedersen, L. Particle mesh Ewald: An N·log(N) method for Ewald sums in large systems *J Chem Phys*. (1993), *98*, 10089-10092.

[44] Ben-Nun, A., Kerlero de Rosbo, N., Kaushansky, N., Eisenstein, M., Cohen, L., Kaye, J.F., *et al.* Anatomy of T cell autoimmunity to myelin oligodendrocyte glycoprotein (MOG): prime role of MOG44F in selection and control of MOG-reactive T cells in H-2b mice. *Eur J Immunol*. (2006), *36*, 478-493.

[45] Ji, N., Somanaboeina, A., Dixit, A., Kawamura, K., Hayward, N.J., Self, C., *et al.* Small molecule inhibitor of antigen binding and presentation by HLA-DR2b as a therapeutic strategy for the treatment of multiple sclerosis. *J Immunol*. (2013), *191*, 5074-5084.

[46] Knapp, B., Fischer, G., Van Hemelen, D., Fae, I., Maillere, B., Ebner, C., *et al.* Association of HLA-DR1 with the allergic response to the major mugwort pollen allergen: molecular background. *BMC immunol*. (2012), *13*, 43.

[47] Stavrakoudis, A. Insights into the structure of the LC13 TCR/HLA-B8-EBV peptide complex with molecular dynamics simulations. *Cell Biochem Biophys*. (2011), *60*, 283-295.

[48] Ferrante, A., Templeton, M., Hoffman, M., Castellini, M.J. The Thermodynamic Mechanism of Peptide-MHC Class II Complex Formation Is a Determinant of Susceptibility to HLA-DM. *J Immunol*. (2015), *195*, 1251-1261.

[49] Wolfson, M.Y., Nam, K., Chakraborty, A.K. The effect of mutations on the alloreactive T cell receptor/peptide-MHC interface structure: a molecular dynamics study. *J Phys Chem B*. (2011), *115*, 8317-8327.

[50] Yaneva, R., Springer, S., Zacharias, M. Flexibility of the MHC class II peptide binding cleft in the bound, partially filled, and empty states: a molecular dynamics simulation study. *Biopolymers*. (2009), *91*, 14-27.

[51] Roe, D.R., Cheatham, T.E. PTRAJ and CPPTRAJ: Software for Processing and Analysis of Molecular Dynamics Trajectory Data. *J Chem Theory Comput*. (2013), *9*, 3084-3095.

[52] Shao, J.Y., Tanner, S.W., Thompson, N., Cheatham, T.E. Clustering molecular dynamics trajectories: 1. Characterizing the performance of different clustering algorithms. *J Chem Theory Comput*. (2007), *3*, 2312-2334.

[53] Albouz-Abo, S., Wilson, J.C., Bernard, C.C., von Itzstein, M. A conformational study of the human and rat encephalitogenic myelin oligodendrocyte glycoprotein peptides 35-55. *Eur J Biochem*. (1997), *246*, 59-70.

[54] Ntountaniotis, D., Vanioti, M., Kordopati, G.G., Kellici, T.F., Marousis, K.D., Mavromoustakos, T., *et al.* A combined NMR and molecular dynamics simulation study to determine the conformational properties of rat/mouse 35-55 myelin oligodentrocyte glycoprotein epitope implicated in the induction of experimental autoimmune encephalomyelitis. *J-Biomol Struct-Dyn*. (2016).

[55] MacArthur, M.W., Thornton, J.M. Influence of proline residues on protein conformation. *J Mol Biol*. (1991), *218*, 397-412.